esa

ECOSPHERE

DISEASE ECOLOGY

Disease and climate effects on individuals drive post-reintroduction population dynamics of an endangered amphibian

MAXWELL B. JOSEPH[1],† AND ROLAND A. KNAPP[2]

[1]*Earth Lab, University of Colorado, Boulder, Colorado 80303 USA*
[2]*Sierra Nevada Aquatic Research Laboratory, University of California, Mammoth Lakes, California 93546 USA*

Citation: Joseph, M. B. and R. A. Knapp. 2018. Disease and climate effects on individuals drive post-reintroduction population dynamics of an endangered amphibian. Ecosphere 9(11):e02499. 10.1002/ecs2.2499

Abstract. The emergence of novel pathogens often has dramatic negative effects on previously unexposed host populations. Subsequent disease can drive populations and even species to extinction. After establishment in populations, pathogens can continue to affect host dynamics, influencing the success or failure of species recovery efforts. However, quantifying the effect of pathogens on host populations in the wild is challenging because individual hosts and their pathogens are difficult to observe. Here, we use long-term mark–recapture data to describe the dynamics of reintroduced populations of an endangered amphibian (*Rana sierrae*) and evaluate the success of these recovery efforts in the presence of a recently emerged pathogen, the amphibian chytrid fungus *Batrachochytrium dendrobatidis*. We find that high *B. dendrobatidis* infection intensities are associated with increases in frog detectability and reductions in survival. When average infection intensities are high, adults are more likely to gain infections and less likely to lose infections. We also find evidence for intensity-dependent survival, with heavily infected individuals suffering higher mortality. These results highlight the need in disease ecology for probabilistic approaches that account for uncertainty in infection intensity using imperfect observational data. Such approaches can advance the understanding of disease impacts on host population dynamics, and in the current study will improve the effectiveness of species conservation actions.

Key words: *Batrachochytrium dendrobatidis;* host–pathogen dynamics; mark–recapture; mountain yellow-legged frog; population establishment; recruitment; reintroduction; survival.

Received 27 May 2018; revised 4 September 2018; accepted 3 October 2018. Corresponding Editor: Allison M. Gardner.

† **E-mail:** maxwell.b.joseph@colorado.edu

INTRODUCTION

Amphibians are one of the most threatened groups of vertebrates (Wake and Vredenburg 2008). Although the drivers of amphibian decline vary taxonomically and spatially, the amphibian chytrid fungus *Batrachochytrium dendrobatidis* (Bd) is a major cause of population declines and species extinctions in montane habitats worldwide (Skerratt et al. 2007, Fisher et al. 2009, Grant et al. 2016). In the face of these declines, species recovery will often require introductions to restore extirpated populations, but little is known about the dynamics of population establishment and persistence of threatened amphibians (Armstrong and Seddon 2008), especially in the presence of disease. Given Bd's role in eliminating populations, we expect introduction outcomes to be shaped by disease impacts on demographic rates, but measuring such impacts in wild populations is difficult (McCallum and Dobson 1995, Briggs et al. 2010).

The mountain yellow-legged frog is emblematic of global amphibian declines. Although

formerly abundant in the relatively protected habitats of California's Sierra Nevada mountains (USA), the two species that make up this taxon (*Rana muscosa* and *Rana sierrae* (Vredenburg et al. 2007)) have disappeared from over 93% of historical localities, due primarily to the introduction of nonnative fish into fishless habitats (Knapp and Matthews 2000, Knapp 2005) and the emergence of Bd (Vredenburg et al. 2010). In response, both species are listed as "endangered" under the U.S. Endangered Species Act and included on the International Union for Conservation of Nature Red List of Threatened Species (IUCN 2017). *R. sierrae* has shown recent signs of recovery in the best-protected portion of its range, including Yosemite National Park, but due to dispersal limitations, the re-establishment of populations may require introductions in addition to natural recovery (Knapp et al. 2016). The effectiveness of such actions remains unclear, and the drivers of post-introduction population dynamics and introduction success or failure are poorly understood.

Introduction outcomes may be described in terms of survival, recruitment, and abundance trajectories. Mark–recapture studies provide a method to estimate these quantities in wild populations while accounting for factors that can complicate inference, including imperfect detection (Jolly 1965, Pradel 1996), multiple classes within the population that may be imperfectly resolved (Lebreton and Cefe 2002, Conn and Cooch 2009), and incompletely observed individual-level traits (Royle 2009). This flexibility is critical for understanding disease impacts in wild populations. Multi-state mark–recapture methods have been applied with great success to understand the population-level impacts of Bd, and differences in demographic rates between infected and uninfected classes (Murray et al. 2009, Pilliod et al. 2010, Sapsford et al. 2015, Hudson et al. 2016).

Assuming that survival depends only on whether an individual is infected, and not considering infection intensity (i.e., load), could be problematic given that Bd-caused frog mortality is often a function of load (Briggs et al. 2010). However, individual-level infection data are often not available. For example, Bd load may not be observed if an individual is not encountered or captured on a survey, or if they are captured but no infection data are collected. This presents a major challenge: Infection intensity is hard to measure, but may be critical for understanding population dynamics. Previous efforts to understand disease impacts in wild populations as a function of load at the individual level have randomly imputed missing infection load data with the observed distribution of load values (Spitzen-van der Sluijs et al. 2017). However, random imputation could bias inference if load data are not missing at random, for example, if heavily infected individuals are easier or more difficult to detect than individuals with lower loads.

In this paper, we seek to understand whether introduction outcomes can be explained by post-introduction disease dynamics or climatic conditions. We expected that failed introductions might be attributed to some combination of disease dynamics that inhibit population growth and climatic conditions that do not favor adult survival or recruitment. We use a Bayesian multi-state model with data from decade-long mark–recapture studies in two reintroduced frog populations. We find that Bd affects introduction success via impacts on adult survival. Winter severity also appears to regulate adult survival and recruitment. In addition, we find that infected adults are easier to detect, which raises broader questions about understanding disease impacts in wild populations and highlights the importance of accounting for hidden individual-level infection dynamics. These insights will inform ongoing and future efforts aimed at restoring the endangered mountain yellow-legged frog and provide a means to quantitatively assess why some introduction efforts fail and others succeed.

Methods

Field sites and methods

The two study lakes are located in eastern Yosemite National Park (California, USA) at elevations of 2880 and 3200 m. *R. sierrae* populations in both lakes were established via translocation from a single nearby donor population (elevation: 3176 m). The donor population has been Bd positive for at least two decades (Fellers et al. 2001), and contains one of the largest *R. sierrae* populations in Yosemite (minimum population size during this study: 600–1500 adults). The introduction lakes are located 5.5–7.0 km from the donor population and both contain high-quality *R. sierrae* habitat (i.e., fishless, 6–12 m deep, with adjacent meadow and stream habitats) (Knapp 2005).

Because these lakes harbor a sensitive species, we refer to them by the pseudonyms Alpine and Subalpine (Lindenmayer and Scheele 2017). At Alpine in the year 2001, five years prior to the translocation of adults into this lake, a single large adult *R. sierrae* was detected on a visual encounter survey (Knapp 2005). No *R. sierrae* of any life stage was detected at Alpine on a visual encounter survey conducted three weeks prior to translocation in 2006. At Subalpine, a single *R. sierrae* tadpole was observed on a visual encounter survey in 2001, seven years prior to adult translocations in 2008. Subsequent surveys in 2005 and 2007 did not detect *R. sierrae* of any life stage at Subalpine. Based on these observations and the widespread historical occurrence of *R. sierrae* across similar lakes in Yosemite, we assumed that both lakes were historically occupied by *R. sierrae* and that these populations were extirpated prior to this study's translocations by the introduction of nonnative fish prior to 1977 and the arrival of Bd in the 1980s or 1990s based on historical declines of *R. sierrae* observed at that time (Phillips 1990, Sherman and Morton 1993, Drost and Fellers 1996).

Prior to translocations, the presence or absence of Bd at these sites was uncertain. It was thought that Bd was likely present at both Alpine and Subalpine, as Bd was ubiquitous or nearly so in Yosemite at that time (Knapp et al. 2011). Both sites and/or adjacent habitats contained other amphibians (Alpine lake: Yosemite toad *Anaxyrus canorus*; Subalpine lake: *A. canorus* and Pacific treefrog *Hyliola regilla*), but the infection status of those species was unknown. It was decided in collaboration with Yosemite National Park that reintroduced *R. sierrae* populations would need to persist in the presence of Bd, because preventing individuals from becoming infected was not feasible, and there was no known means to eliminate Bd from the environment. The potential risk associated with introducing Bd or a novel strain of Bd to these sites was determined to be low relative to the benefits associated with re-establishing populations of *R. sierrae*.

The initial introduction of frogs to Alpine and Subalpine occurred during summer 2006 and 2008, respectively, and additional introductions to supplement both populations were conducted in subsequent years. Prior to introduction, adult frogs (≥40 mm snout–vent length [SVL]) were captured at the donor site, and tagged (8 mm passive integrated transponder [PIT] tags), measured, and weighed. To estimate Bd load, we also collected a skin swab from each frog using standard methods (Hyatt et al. 2007, Vredenburg et al. 2010). In the first introduction to Alpine, frogs were transported on foot; in all subsequent introductions to both Alpine and Subalpine, frogs were transported via helicopter. The number of individuals introduced to each study site on each introduction date is provided in Table 1.

To describe the dynamics of the introduced populations, both populations were assessed for 10–12 yr using mark–recapture methods. Between 2006 and 2012, lakes were visited approximately once per month during the summer active season (June–September) and on a single day (primary period) all habitats were searched repeatedly for frogs which were captured using handheld nets. Adult frogs were identified via their PIT tag (or tagged if they were untagged), measured, weighed, swabbed, and released at the capture location. During 2013–2017, we adopted a robust design in which all habitats were searched during several consecutive days (surveys), and frogs processed as described above. Within a primary period, frogs that were captured on more than one survey were measured, weighed, and swabbed only when first captured.

Skin swabs were analyzed using standard Bd DNA extraction and qPCR methods (Boyle et al. 2004) except that swab extracts were analyzed singly instead of in triplicate (Kriger et al. 2006, Vredenburg et al. 2010). During 2005–2014, we used standards developed from known concentrations of zoospores (Boyle et al. 2004), and after 2014, we used standards based on single ITS1 PCR amplicons (Longo et al. 2013). Based on paired comparisons between samples analyzed using both types of standards, Bd in the study

Table 1. Schedule of frog introductions to the study lakes.

Lake	Year	Number of frogs
Alpine	2006	40
	2013	20
Subalpine	2008	36
	2013	19
	2015	20
	2017	30

area has an average of 60 ITS1 copies per zoospore. To express all qPCR results as the number of ITS1 copies, starting quantities obtained using the zoospore standard (measured as "zoospore equivalents") were multiplied by 60. In addition, all qPCR quantities (regardless of standard) were multiplied by 80 to account for the fact that DNA extracts from swabs were diluted 80-fold during extraction and PCR (Vredenburg et al. 2010).

We acquired hourly air temperature and daily snow depth data from two nearby meteorological stations (ERY and DAN, respectively) and snow water equivalent data from a manually measured snow course (DAN; California Data Exchange Center—http://cdec.water.ca.gov). The stations and snow course are 5–17 km from the study lakes. We used snow water equivalent as measured on 1 April of each year as a measure of winter severity, to be used as a covariate for frog recruitment and survival. Daily snow depth data were acquired to model survey occurrence as described below. To better understand the detection process, we averaged hourly air temperature data collected between 09:00 and 16:00 hours on each day a survey took place, to derive a "survey air temperature" metric.

Model development

We developed a hierarchical Bayesian hidden Markov model to understand how environmental factors and partly observed time-varying individual traits (Bd loads) jointly drive population dynamics. This model also needed to account for the partly deterministic recruitment process that arises with introductions. The result is an extended open population Jolly-Seber mark–recapture model with known additions to the population (introduced adults), continuous uncertain infection states of individuals which may or may not be captured, and sampling that is unevenly distributed in time.

In a small number of cases, adults were captured, weighed, and measured, but no swab data were associated with the capture (e.g., if a swab was lost). In these cases (81 of 2697 swabs), capture data indicate that the adult was alive during the survey, but its infection status is unknown. As such, there are three possible observations for captured frogs: detected/infected, detected/uninfected, and detected/unknown infection status. A fourth possible observation class corresponds to non-detection: An individual was not observed during a survey.

Mark–recapture model structure

We consider four possible observations for each individual $i = 1, \ldots, M$ on each survey $j = 1, \ldots, n_j$: $o_{i,j} = 1$ indicates that the individual was not detected; $o_{i,j} = 2$ indicates that the individual was observed and the swab collected for that individual indicated that they were uninfected; $o_{i,j} = 3$ indicates that the individual was observed and results from the collected swab showed that the frog had a non-zero Bd load; and $o_{i,j} = 4$ indicates that the individual was observed, but no swab data were available from the capture.

We use parameter-expanded data augmentation to account for the fact that the total number of adults in the population is unknown (Royle and Dorazio 2012). Across the entire time period of the study, we assume N_s individuals have existed in the population, comprising the superpopulation of individuals that were present at some time. While N_s is not directly observable, across all surveys $n \leq N_s$ unique individuals were known to be present in the population (because they were introduced and/or captured). An estimate of N_s can be acquired by considering a large number $M > N_s$ of individuals, $M - N_s$ of which never existed (Royle 2009). Thus, the model has a state corresponding to individuals that have not recruited yet. Here, M was chosen to be 2218 at Alpine (618 observed unique individuals plus 1600 augmented individuals) and 558 at Subalpine (158 observed individuals and 400 augmented individuals). These values were chosen to be considerably greater than our prior guess of N_s, and we also verified that posterior estimates of N_s were much less than M to avoid problems on the boundary of this augmented parameter space (Dennis et al. 2015).

We denote the true state of individual i in primary period t as $u_{i,t}$, for every individual $i = 1, \ldots, M$ and each primary period $t = 1, \ldots, n_t$. The four states that we consider are as follows: $u_{i,t} = 1$ for individuals that have not recruited, $u_{i,t} = 2$ for uninfected adults, $u_{i,t} = 3$ for infected adults, and $u_{i,t} = 4$ for dead individuals. Each survey $j = 1, \ldots, n_j$ occurs in one of the n_t primary periods, and we denote the primary period in which survey j takes place as t_j. Each primary period t occurs within one year, but within a year

there are multiple primary periods. We set the year containing the first primary period to $y_{t=1} = 1$, and generally, y_t represents the year containing primary period t. Years increment by 1 until the final year of the mark–recapture efforts, which we denote n_y: $y \in \{1, 2, \ldots, n_y\}$. We assume that within a primary period, the state of each individual does not change (i.e., individuals do not recruit into the adult population, gain or lose Bd infection, or die). This assumption is justified by the short time intervals between surveys within primary periods.

Observation model.—An emission matrix $\mathbf{\Omega}_{i,j}$ links observations to hidden states, with the elements of $\mathbf{\Omega}_{i,j}$ providing the probability of each possible observation of individual i in survey j, given the true hidden state. The rows in $\mathbf{\Omega}_{i,j}$ correspond to the state of individual i in primary period t_j, and the columns correspond to an observation of individual i in survey j:

$$\Omega_{i,j} = \begin{array}{c} \begin{array}{cccc} \text{Not detected} & \text{Bd negative} & \text{Bd positive} & \text{Bd unknown} \\ o_{i,j}=1 & o_{i,j}=2 & o_{i,j}=3 & o_{i,j}=4 \end{array} \\ \begin{pmatrix} 1 & 0 & 0 & 0 \\ 1-p_{i,j}^{-} & p_{i,j}^{-}\delta & 0 & p_{i,j}^{-}(1-\delta) \\ 1-p_{i,j}^{+} & 0 & p_{i,j}^{+}\delta & p_{i,j}^{+}(1-\delta) \\ 1 & 0 & 0 & 0 \end{pmatrix} \end{array} \begin{array}{c} \text{Not recruited} \\ u_{i,t_j}=1 \\ \text{Uninfected} \\ u_{i,t_j}=2 \\ \text{Infected} \\ u_{i,t_j}=3 \\ \text{Dead} \\ u_{i,t_j}=4 \end{array}$$

The structure of $\mathbf{\Omega}_{i,j}$ implies that there are no mistaken individual identifications (those that are dead or not recruited are never detected) and that a swab successfully makes it to the laboratory and provides qPCR data with probability δ, conditional on the animal being detected. Detection probabilities are provided by $p_{i,j}^{-}$ for uninfected (Bd negative) and $p_{i,j}^{+}$ for infected (Bd positive) individuals, and these detection probabilities can vary by individual and survey. We also assume that there are no false-positive or false-negative Bd results (Hyatt et al. 2007), though relaxing this assumption may be a promising future area, given the potential sensitivity of swab results to infection intensity (Miller et al. 2012).

State model.—The hidden states of each individual evolve as a Markov process with transition matrix $\mathbf{\Psi}_{i,t}$, the entries of which provide the probability of transitioning to state $u_{i,t+1}$ (the column index) from state $u_{i,t}$ (the row index). This matrix is different for individuals that naturally recruit vs. those that recruit deterministically due to introduction. For naturally recruiting individuals:

$$\mathbf{\Psi}_{i,t} = \begin{array}{c} \begin{array}{cccc} \text{Not recruited} & \text{Uninfected} & \text{Infected} & \text{Dead} \\ u_{i,t+1}=1 & u_{i,t+1}=2 & u_{i,t+1}=3 & u_{i,t+1}=4 \end{array} \\ \begin{pmatrix} 1-\lambda_t & \lambda_t(1-\gamma_t) & \lambda_t\gamma_t & 0 \\ 0 & \phi_{i,t}^{-}(1-\eta_t^{+}) & \phi_{i,t}^{-}\eta_t^{+} & 1-\phi_{i,t}^{-} \\ 0 & \phi_{i,t}^{+}\eta_t^{-} & \phi_{i,t}^{+}(1-\eta_t^{-}) & 1-\phi_{i,t}^{+} \\ 0 & 0 & 0 & 1 \end{pmatrix} \end{array} \begin{array}{c} \text{Not recruited} \\ u_{i,t}=1 \\ \text{Uninfected} \\ u_{i,t}=2 \\ \text{Infected} \\ u_{i,t}=3 \\ \text{Dead} \\ u_{i,t}=4 \end{array}$$

where λ_t is the probability that an individual enters the adult population between primary periods t and $t + 1$, γ_t is the probability that a recruiting individual is infected conditional on entry, $\phi_{i,t}^{-}$ is a survival probability for an uninfected adult, $\phi_{i,t}^{+}$ is a survival probability for an infected adult, η_t^{+} is the probability of transitioning from the uninfected to infected class conditional on survival, and η_t^{-} is the probability of transitioning from the infected to uninfected class conditional on survival.

For introduced individuals, the recruitment process is deterministic. Specifically, for each introduced adult, there is zero chance that they recruit prior to the primary period in which they are introduced, and if they are introduced at time t_i^{intro}, then the probability that they recruit into a particular class (their state upon introduction) must be 1. For these introductions, all introduced adults were infected, and thus recruited into the infected adult class, leading to the following transition matrix for introduced animals, where the recruitment process is completely determined by t_i^{intro}, such that $\mathbf{\Psi}_{i,t}$ is:

$$\begin{array}{c} \begin{array}{cccc} \text{Not recruited} & \text{Uninfected} & \text{Infected} & \text{Dead} \\ u_{i,t+1}=1 & u_{i,t+1}=2 & u_{i,t+1}=3 & u_{i,t+1}=4 \end{array} \\ \begin{pmatrix} 1-I_{(t=(t^{\text{intro}}{}_i-1))} & 0 & I_{(t=(t^{\text{intro}}{}_i-1))} & 0 \\ 0 & \phi_{i,t}^{-}(1-\eta_t^{+}) & \phi_{i,t}^{-}\eta_t^{+} & 1-\phi_{i,t}^{-} \\ 0 & \phi_{i,t}^{+}\eta_t^{-} & \phi_{i,t}^{+}(1-\eta_t^{-}) & 1-\phi_{i,t}^{+} \\ 0 & 0 & 0 & 1 \end{pmatrix} \end{array} \begin{array}{c} \text{Not recruited} \\ u_{i,t}=1 \\ \text{Uninfected} \\ u_{i,t}=2 \\ \text{Infected} \\ u_{i,t}=3 \\ \text{Dead} \\ u_{i,t}=4 \end{array}$$

where $I_{(t=(t_i^{\text{intro}}-1))}$ is an indicator function equal to 1 when t is equal to $t_i^{\text{intro}} - 1$.

An imaginary first primary period augments the collection of primary periods when introductions took place and when surveys occurred, and was set to occur one week before the initial introductions into each population. For this augmented period $t = 1$, we assume that all individuals are in the "not-recruited" class, $u_{i,1} = 1$ for $i = 1, \ldots, M$ (Fig. 1). Given that neither lake was known to contain adult frogs immediately prior to introduction, this is potentially a fair assumption, but in case the assumption was violated and adults were present prior to the introduction, we include a time-varying adjustment into the recruitment model (see 2. *Recruitment probabilities*).

The number of primary periods was not uniform across survey years, and as such, the time between primary periods was also heterogeneous, complicating the interpretation of transition probabilities. Thus, at both sites, we used augmented primary periods to increase the regularity of time intervals between primary periods. These were chosen to occur when primary periods might have occurred, for example, not during the winter months when the lakes are snow-covered, using a statistical model of when surveys are conducted. At each site, we fit a binomial generalized additive model with thin plate spline smoothers for day of year and daily snow depth at Dana Meadows, where the response variable was 0 or 1 for each day, with 1 indicating that a survey took place. These models were fit using the `gam` function in the mgcv package in the R programming language (R Core Team 2017, Wood 2017). Then, we predicted new values from these models, with the goal of augmenting the set of primary periods for each year at each site until all years except the first and last had the same number of primary periods (the maximum number of primary periods within one year at each site: ten at Alpine and eight at Subalpine). Augmented primary periods were only accepted if there was no primary period within five days (before and after) of the proposed augmented primary period. The end result is a set of primary periods that are more uniformly distributed in time than the original collection of empirical primary periods, though these augmented primary periods are not associated with real surveys.

Parameter model.—1. Detection probabilities.— Among uninfected adult frogs, we assume that the probability of detection varies with survey air temperature (Sinsch 1984), so that

$$\text{logit}(p_{i,j}^{-}) = \alpha^{(p)} + \beta^{(p,x)} x_j,$$

where $\alpha^{(p)}$ is an intercept parameter, $\beta^{(p,x)}$ is the effect of survey air temperature on detection probability, and x_j is the survey air temperature for survey j, for all i, j. Among infected adult frogs, the detection model was expanded to allow for an adjustment to account for being

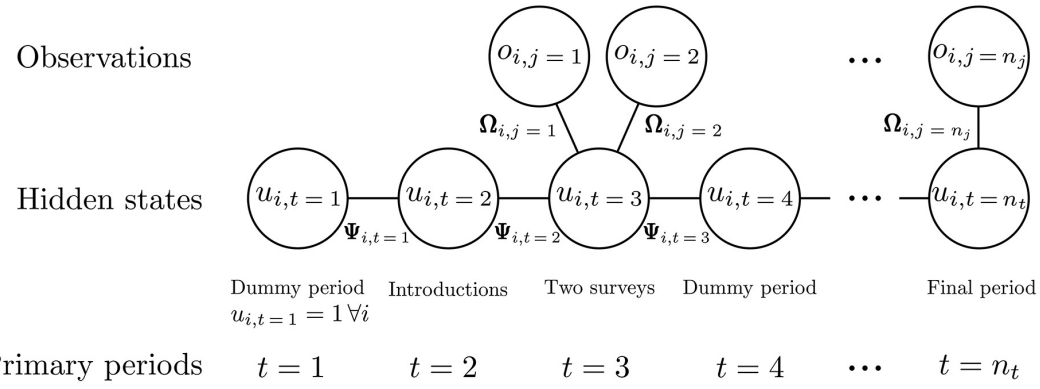

Fig. 1. Summary of hidden Markov model structure. On the first primary period $t = 1$, we assume that all individuals $i = 1, \ldots, M$ are in the not-recruited class. The second primary period represents the first introduction. In this example, two surveys $j = 1, 2$ are conducted on the third primary period. The fourth primary period is a dummy period, inserted to increase the regularity of time intervals between primary periods, and has no associated surveys.

infected, and a further adjustment to deal with variation due to Bd load:

$$\text{logit}(p^{+}_{i,j}) = \alpha^{(p)} + \beta^{(p,x)}x_j + \beta^{(p,+)} + \beta^{(p,z)}z_{i,t_j},$$

where $\beta^{(p,+)}$ is the adjustment on the intercept for infected adults and $\beta^{(p,z)}$ is a coefficient for the log Bd load z_{i,t_j} of individual i in primary period t containing survey j, for all i, j.

2. Recruitment probabilities.—The recruitment model was designed to account for annual variation in Bd loads, whether primary periods spanned years, and winter severity. For the probability of entering the population between primary period t and $t + 1$, we have:

$$\text{logit}(\lambda_t) = \alpha^{(\lambda)} + \beta^{(\lambda,w)}w_t + \beta^{(\lambda,s)}s_{y_t} + \beta^{(\lambda,1)}I_{(t=1)} + \epsilon^{(\lambda)}_{y_t},$$

where $\alpha^{(\lambda)}$ is an intercept term, and the effect of an overwinter transition is represented as $\beta^{(\lambda,w)}$, with w_t as a binary indicator of whether a transition from period t to $t + 1$ spans a winter (or equivalently, two years). The effect of the previous winter's severity is $\beta^{(\lambda,s)}$, where s_{y_t} is previous winter's severity. The parameter $\beta^{(\lambda,1)}$ is an adjustment for the recruitment probability after the first imaginary primary period, which could account for undetected individuals present prior to introduction. Finally, $\epsilon^{(\lambda)}_{y_t}$ is an adjustment to account for extra annual variation. The probability that an individual is infected, conditional on recruitment, is modeled as a function of expected Bd load among infected adults:

$$\text{logit}(\gamma_t) = \alpha^{(\gamma)} + \beta^{(\gamma,\mu)}\mu_{y_t} + \epsilon^{(\gamma)}_{y_t},$$

where $\alpha^{(\gamma)}$ is an intercept, $\beta^{(\gamma,\mu)}$ represents the effect of mean Bd load among infected adults in the year containing primary period t (denoted μ_{y_t}), and $\epsilon^{(\gamma)}_{y_t}$ is a year-specific adjustment.

3. Survival probabilities.—Survival of uninfected adults was modeled as a function of whether a transition spanned an overwinter period and winter severity:

$$\text{logit}(\phi^{-}_{i,t}) = \alpha^{(\phi^-)} + \beta^{(\phi^-,w)}w_t + \beta^{(\phi^-,s)}s_{y_t} + \epsilon^{(\phi^-)}_{y_t},$$

where $\alpha^{(\phi^-)}$ is an intercept parameter, $\beta^{(\phi^-,w)}$ is an adjustment for overwinter transitions, $\beta^{(\phi^-,s)}$ is a coefficient for winter severity, and $\epsilon^{(\phi^-)}_{y_t}$ is a year-specific adjustment. The survival probabilities for infected adults were similarly modeled, but with additional effects of individual Bd load:

$$\text{logit}(\phi^{+}_{i,t}) = \alpha^{(\phi^+)} + \beta^{(\phi^+,w)}w_t + \beta^{(\phi^+,s)}s_{y_t} + \beta^{(\phi^+,z)}z_{i,t} + \epsilon^{(\phi^+)}_{y_t},$$

where $z_{i,t}$ is the log-transformed Bd load of individual i during primary period t, $\beta^{(\phi^+,z)}$ is a coefficient for Bd load, and the remainder of parameters are defined using the same notation as for the survival of uninfected adults.

4. Loss- and gain-of-infection probabilities.—The probability that an infected adult loses infection was modeled as a function of mean Bd load in the infected population, and whether a transition occurred from one year to the next:

$$\text{logit}(\eta^{-}_{t}) = \alpha^{(\eta^-)} + \beta^{(\eta^-,\mu)}\mu_{y_t} + \epsilon^{(\eta^-)}_{y_t},$$

where $\alpha^{(\eta^-)}$ is an intercept, $\beta^{(\eta^-,\mu)}$ is the effect of expected Bd load among infected adults, and $\epsilon^{(\eta^-)}_{y_t}$ is a year-specific adjustment. Transitions from the uninfected to infected class were modeled similarly:

$$\text{logit}(\eta^{+}_{t}) = \alpha^{(\eta^+)} + \beta^{(\eta^+,\mu)}\mu_{y_t} + \epsilon^{(\eta^+)}_{y_t}$$

where parameter notation conventions and definitions match those for transitions from the infected to uninfected classes.

5. Bd loads.—The fact that individuals are imperfectly detected, and that occasionally, individuals are detected but no infection data are collected, presents a challenge for including individual-level Bd loads in the model. Within the infected population, Bd loads are partially observed when individuals are captured and swabs are collected. We used a normal distribution to represent (potential) log Bd loads:

$$[\mathbf{Z}|\mu,\sigma] = \prod_{i=1}^{M}\prod_{t=1}^{n_t}\text{Normal}(z_{i,t}|\mu_{y_t},\sigma)$$

When the load of individual i during primary period t was observed, this specifies a likelihood. Otherwise, this specifies a prior distribution for the potential log load of individual i on primary period t, conditional on infection. The expected value of Bd load among infected adults was assumed to vary among years, and potentially vary as a function of winter severity:

$$\left[\mu|\alpha^{(\mu)},\beta^{(\mu)},\sigma^{(\mu)}\right]=\prod_{y=1}^{n_y}\text{Normal}(\mu_y|\alpha^{(\mu)}+\beta^{(\mu)}s_y,\sigma^{(\mu)})$$

6. Prior distributions.—Based on knowledge of the observation process, we expected that most captures resulted in a non-missing swab result, leading to the specification for the prior on δ as $[\delta]=\text{Beta}(\delta|9,1)$. Annual adjustments were modeled using zero-mean normal distributions with unknown standard deviations specific to the process of interest, for example, for the probability of entering the population: $\left[\epsilon^{(\lambda)}\right]=\prod_{y=1}^{n_y}\text{Normal}(\epsilon_y^{(\lambda)}|0,\sigma^{(\epsilon^{(\lambda)})})$. Standard deviation parameters were given half-normal priors, that is, $\left[\sigma^{(\epsilon^{(\lambda)})}\right]=\text{Normal}_+(\sigma^{(\epsilon^{(\lambda)})}|0,1.5)$, and all the remaining parameters were given Normal(0, 1.5) priors. The full factorization of the joint distribution of data and parameters is provided in Appendix S1: Joint distribution factorization.

7. Parameter estimation.—We implemented the model in Stan, a probabilistic programming language, and sampled from the approximate posterior distribution of parameters with automatic differentiation variational inference (Kucukelbir et al. 2015, Carpenter et al. 2016). We used the forward algorithm (Zucchini et al. 2016) to circumvent the need to sample from the discrete space of true individual states (see Appendix S2: Forward algorithm description for details). Variational inference uses a simple family of distributions as an approximation of the posterior distribution, optimizing parameters of this simpler approximation (the variational distribution) to minimize the Kullback-Leibler divergence between the true posterior and the variational distribution. A variational approximation was necessary for the models to run in a reasonable amount of time (≈2–4 h) on finite resources (r4.2xlarge EC2 instances on Amazon Web Services, with eight virtual CPUs and 61 GiB RAM). To verify our model implementation, we simulated data with known parameters from the model to evaluate parameter recovery and check that parameters were identifiable. These simulations allowed us to identify a lack of identifiability in an earlier model specification which included multiplicative interaction terms between winter severity and Bd load for both the probability of entering the population and the probability that new adults were infected conditional on recruitment.

All code and data necessary to reproduce the analysis and manuscript are publicly available at https://www.github.com/snarl1/sierra-reintroduction-cmr (Joseph and Knapp 2018). The workflow is wrapped into GNU Make command (Stallman et al. 2004), the manuscript is written in R Markdown (Allaire et al. 2018), and we used the R programming language (R Core Team 2017) with the assertthat, ggrepel, ggridges, ggthemes, lubridate, mgcv, patchwork, reshape2, rstan, and tidyverse packages to facilitate data processing, model fitting, and visualization (Wood 2004, Wickham 2007, 2017*a*, *b*, Grolemund and Wickham 2011, Stan Development Team 2016, Pedersen 2017, Slowikowski 2017, Arnold 2018, Wilke 2018). The computational environment with these dependencies is containerized via Docker, and the Dockerfile for the image exists in the GitHub repository for this project (Boettiger 2015).

Results

Detection probabilities

At both sites, infected adults were easier to detect than uninfected adults, and detection probabilities also increased with survey air temperature (Fig. 2A). For a survey with an air temperature of 17°C, the estimated probability of detecting an uninfected adult at Alpine was 0.157 (0.15, 0.163; posterior median and 90% credible intervals [CI]), but for an infected adult with average Bd load, the probability of detection was 0.324 (0.306, 0.34). At Subalpine, for a survey with the same air temperature, the probability of detecting an uninfected adult was 0.19 (0.17, 0.211), but the probability of detecting an infected adult with an average Bd load was 0.598 (0.551, 0.646). Among infected adults, there was evidence for additional increases in detectability with increases in Bd load in the Alpine population (posterior median for $\beta^{(p,z)}$: 0.107, 90% CI: 0.086, 0.129) but not in the Subalpine population ($\beta^{(p,z)}$: 0.001, 90% CI: −0.056, 0.053) (Fig. 2B).

Infection dynamics

Despite the two study populations being 12 km apart, mean Bd loads among infected

adults varied synchronously between populations. After initial introduction in 2006 or 2008, mean loads at both sites were typically between 1000 and 10,000 copies, with a reduction in mean Bd load during the year following the first introduction (Fig. 3A). Thereafter, loads were relatively low and stable through 2012. At both sites, mean loads were uncharacteristically low in 2013 but increased in subsequent years until reaching a peak in 2016. Mean Bd loads at Subalpine tended to be higher than at Alpine, particularly in the period 2015–2017. The estimated correlation over time between mean log Bd loads at the two study sites was 0.636 (0.315, 0.861) (Fig. 3A). This correlation was not due to a shared response to winter severity because winter severity did not influence Bd load at either site (at Alpine $\beta^{(\mu)}$: −0.12 (−0.604, 0.37); at Subalpine $\beta^{(\mu)}$: −0.022 (−0.909, 0.912)).

At both sites, transitioning from the uninfected to the infected adult class (gaining infection) was more likely than transitioning from the infected to the uninfected class (losing infection) over most of the study period. Among-year variation in transition probabilities was similar at both sites, with 2013 having higher-than-average loss-of-infection probabilities (Fig. 4A). This was most likely due to exceptionally low mean Bd loads in 2013: When Bd loads were low, adults were more likely to lose infection at both study sites, and less likely to gain infection in the Subalpine population (Fig. 4B). As a consequence, when mean Bd loads were high, prevalence also tended to be high (Fig. 3). The correlation between prevalence and mean Bd loads among infected adults was estimated to be 0.322 (0.127, 0.496) at Alpine and 0.392 (0.169, 0.56) at Subalpine.

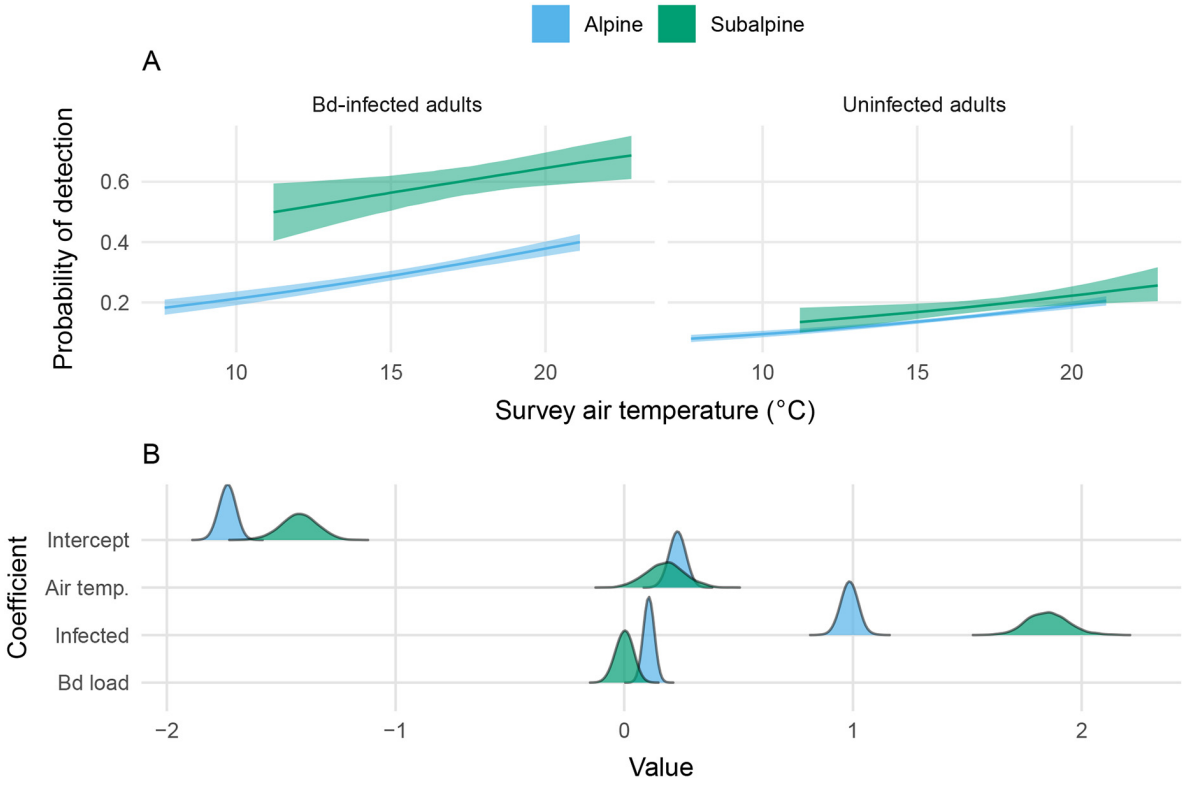

Fig. 2. (A) Estimated detection probabilities as a function of survey air temperature for Bd-infected and uninfected adults. The ribbons represent the 90% posterior credible interval, and the line represents the posterior median. Predictions for Bd-infected adults correspond to individuals with average infection loads at each site. (B) Parameter estimates for the detection model. Each of the detection parameters is shown on the *y*-axis. Color indicates population.

Fig. 3. (A) Bd infection loads over time. Observed load values from skin swabs are shown as points on a log10 scale, colored by site. The estimated average Bd infection load is shown as a line (posterior median) with a 90% credible interval ribbon. (B) Estimated Bd infection prevalence over time, with posterior medians shown as lines and 90% credible intervals shown as shaded ribbons.

Population dynamics

Following initial introduction, both sites experienced multiple years of low abundance, but in 2013 the adult population at Alpine began increasing, reaching values upwards of 400 adults by late summer 2016 (Fig. 5A). In contrast, at Subalpine, the adult population probably has not exceeded 50 individuals over much of the study duration, and introduction events account for the largest recruitment pulses. At both sites, infected adults tended to outnumber uninfected adults throughout the study period. The total number of adults to have ever existed (N_s) was estimated to be 768 (686, 848) at Alpine and 172 (147, 212) at Subalpine.

Infected adults experienced decreased overwinter survival, especially in the Subalpine population, unlike uninfected adults which maintained overwinter survival that was comparable to within-summer survival (Fig. 5B). Bd load reduced infected adult survival at Alpine (Fig. 6), with $\beta^{(\phi^+,z)}$ estimated to be −0.132 (−0.211, −0.045) at Alpine and −0.078 (−0.199, 0.05) at Subalpine. Winter severity appeared to increase survival of Bd-infected adults at Alpine ($\beta^{(\phi^+,s)}$: 0.303 (0.173, 0.436)), but may have been associated with lower survival at Subalpine (−0.239 (−0.465, 0)). At both sites, winter severity coefficients overlapped zero for uninfected adults ($\beta^{(\phi^-,s)}$: −0.044 (−0.735, 0.661) at Alpine and 0.349 (−0.139, 0.842) at Subalpine). Overall, uninfected adults had higher survival at Alpine ($\alpha^{(\phi^-)}$: 4.146 (3.42, 4.883)) than Subalpine ($\alpha^{(\phi^-)}$: 2.183 (1.782, 2.594)) (Fig. 5B).

Introduced adults survived longer on average at Alpine compared to Subalpine (Fig. 7). At the end of the summer following the initial introduction of adults at Alpine, the proportion of adults surviving was 0.825 (0.675, 0.95). At Subalpine, only about half (0.583 (0.385, 0.778)) of adults survived to the end of the first summer following initial introduction. In the year after the initial introduction, the estimated proportion of introduced adults surviving at Alpine was 0.675 (0.45, 0.85), and at Subalpine just 0.306 (0.139, 0.528). Similar differences in survival were evident following subsequent introductions, with low within-summer and among-year survival at Subalpine and a higher survival rate at Alpine (Fig. 7).

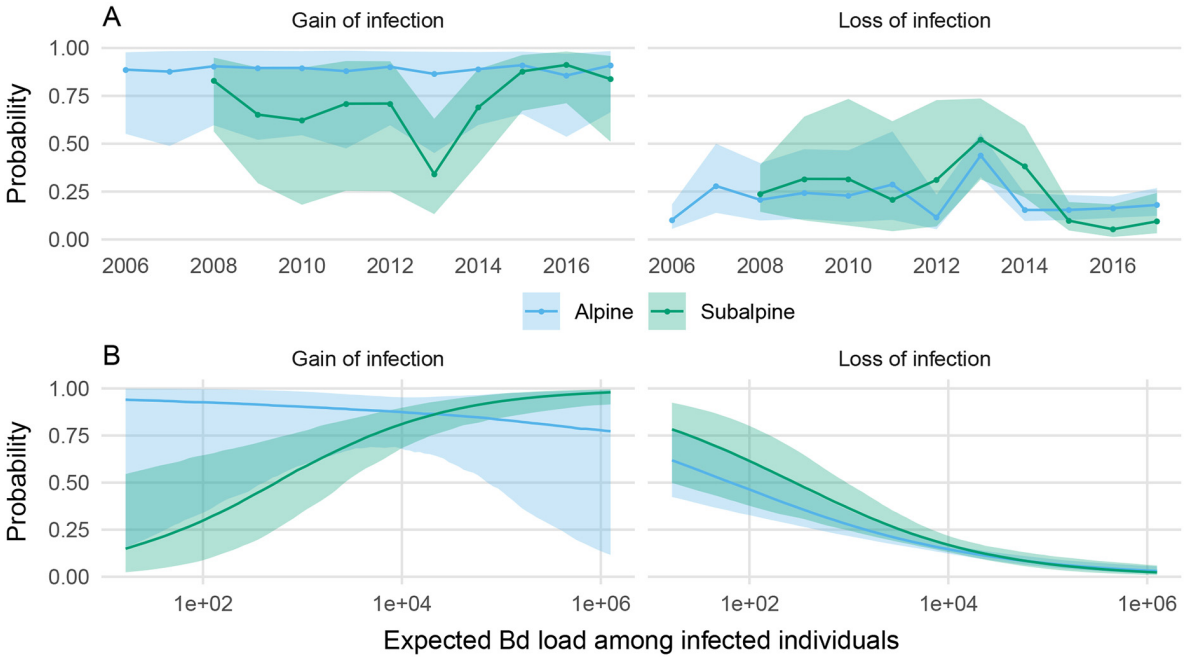

Fig. 4. (A) Estimated transition probabilities between the uninfected and infected adult classes at both sites in each year. Ribbons represent the 90% posterior credible interval, with the midline representing the posterior median. Dots connected by lines represent years. (B) Estimated transition probabilities from the uninfected adult class to the infected adult class and vice versa as a function of expected Bd load among infected adults. The line represents the posterior median, and the ribbons indicate the 95% credible interval, with colors differentiating study sites.

Little to no recruitment was observed during the 3–4 yr following the initial introductions, consistent with the multi-year larval and juvenile stages in this species ("recruitment" is the addition of new adults to the population). However, Alpine experienced large recruitment pulses in 2013, 2014, and 2016 (Fig. 8). The Subalpine population had smaller pulses of recruitment during the period 4–6 yr after the introduction, but little recruitment in subsequent years (Fig. 8). Recruitment pulses were asynchronous between the two populations, particularly in 2016 when a very large pulse of recruits was observed at Alpine but not Subalpine.

Recruitment dynamics varied as a function of winter severity and Bd load. In both populations, winter severity reduced recruitment (at Alpine $\beta^{(\lambda,s)}$: −1.41 (−1.55, −1.264); at Subalpine $\beta^{(\lambda,s)}$: −1.295 (−1.612, −1.001)). Recruitment overwinter (before the first primary period of the year) was less likely than recruitment among within-year primary periods at Alpine ($\beta^{(\lambda,w)}$: −2.763 (−3.946, −1.551)), but more likely at Subalpine ($\beta^{(\lambda,w)}$: 1.677 (1.117, 2.256)). Conditional on entering the population, adults at Alpine were more likely to recruit into the infected class when mean Bd loads were high ($\beta^{(\gamma,\mu)}$: 1.195 (0.356, 2.104)), but mean Bd load was not associated with the probability of recruiting as infected at Subalpine ($\beta^{(\gamma,\mu)}$: −0.575 (−2.199, 1.192)), perhaps due to low recruitment and therefore low power to detect such an effect.

Discussion

The modeling approach developed here provides a quantitative means to assess how climate and disease affect demographic rates and population dynamics in hard-to-sample host populations. This builds on previous research that incorporated individual-level covariates in mark–recapture models (Pledger et al. 2003, Royle 2008, Gimenez and Choquet 2010, Ford et al. 2012) and that evaluated effects of Bd load at the individual level in wild populations

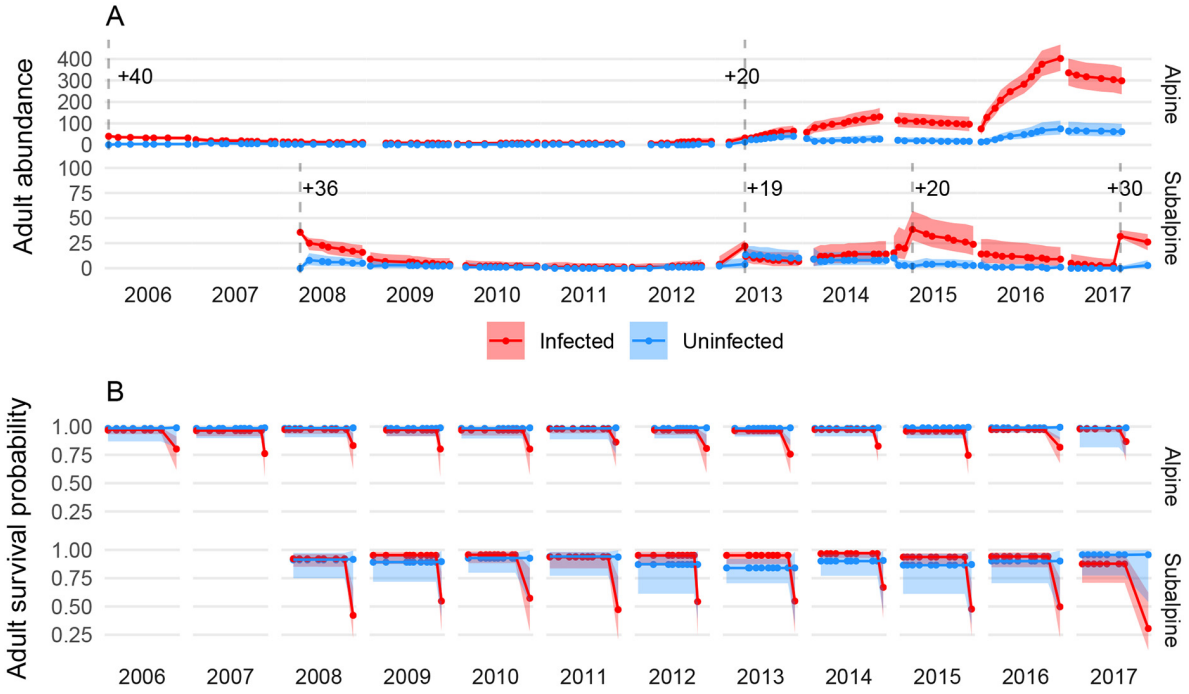

Fig. 5. Estimated abundance (A) and survival (B) time series for infected and uninfected adults at both populations. Time is shown on the *x*-axis, with facets for years. Posterior medians for each primary period are shown as points connected by line segments, and the 90% credible interval is shown as a shaded ribbon. In A, the vertical dashed lines indicate introduction events, and the number of adults added in each event is indicated with a "+" symbol. Also note the difference in the *y*-axis scales between the two sites.

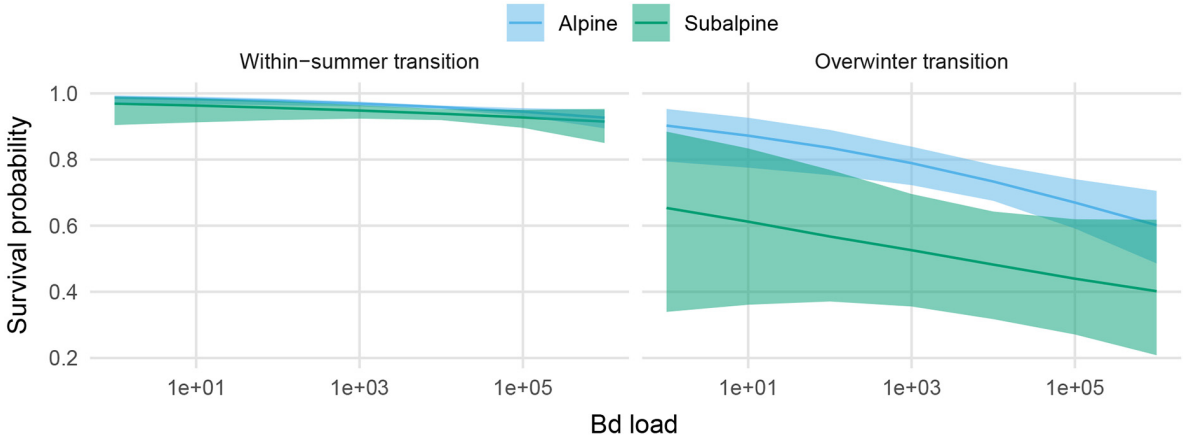

Fig. 6. Estimated survival probabilities for within-summer and overwinter transitions among infected adults as a function of Bd infection load. The *x*-axis shows Bd load over the range of observed values. The *y*-axis represents survival probabilities. Posterior medians are lines, and 90% credible intervals are ribbons.

(Spitzen-van der Sluijs et al. 2017). Our approach is unique in part because we treat unobserved infection status and intensity as parameters, rather than using imputation to backfill missing intensity values. Accounting for uncertainty in individual-level infection intensity in a Bayesian framework simplifies uncertainty propagation to key parameters including detection and survival

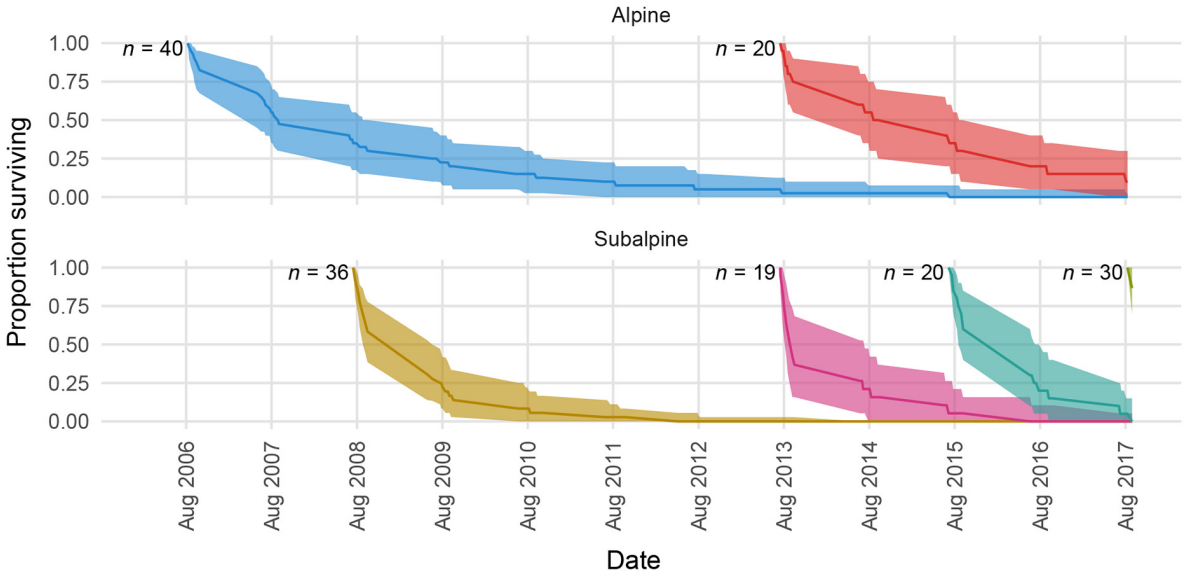

Fig. 7. Estimated survival of introduced adults at both populations, colored by introduction event. Time is shown on the *x*-axis, with the proportion of adults surviving on the *y*-axis. The number of individuals introduced in each introduction event is labeled as $n = \ldots$. The ribbons represent the 90% posterior credible interval, with the midline representing the posterior median.

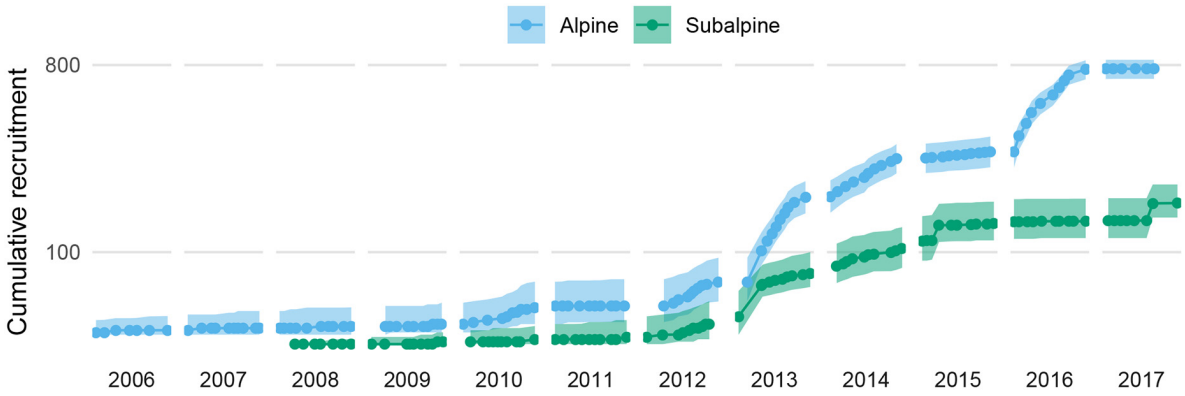

Fig. 8. Estimated cumulative number of natural recruits into the adult population at both sites over time (on a log10 scale). The ribbons represent the 90% posterior credible interval, with the midline representing the posterior median. Dots connected by lines represent primary periods.

probabilities. This may provide a better understanding of how individual traits relate to demographic processes and population dynamics, especially when capture histories are biased by individual infection loads and/or disease.

Overall, results indicated that the introduction of frogs to Alpine was successful in establishing a large self-sustaining population, but unsuccessful at Subalpine. The success of the introduction effort at Alpine seems to be driven by relatively low Bd loads, high adult survival, and large recruitment pulses into the adult population following mild winters. In contrast, the failure of introductions into Subalpine was associated with higher Bd loads, lower adult survival, and smaller, infrequent recruitment pulses. The estimated effect of Bd load on the survival of infected adults was similar in both populations,

but loads on average were higher at Subalpine. Given the negative effect of Bd load on frog survival, the cause of higher loads on frogs at Subalpine is worthy of additional study. In addition, the fact that the effect of Bd load on survival of infected adults was similar in both populations, but loads on average were higher at Subalpine also suggests that the observed introduction outcomes cannot be explained by differences between the two populations in frog tolerance of Bd infection within summer seasons (Råberg et al. 2009, Wilber et al. 2017).

The two study lakes were relatively distant from each other and located in catchments with different environmental characteristics, but despite this, Bd loads were temporally correlated across the two sites. The synchrony in expected load is worth further investigation, as it may indicate environmental forcing of infection dynamics, for example, variation due to temperature (Phillott et al. 2013, Cohen et al. 2017, but see Knapp et al. 2011), or some form of connectivity among sites, although the latter possibility seems unlikely. Future studies might also seek to better disentangle landscape-wide factors driving synchrony and local factors that drive differences in mean load, particularly in the context of known mechanisms of disease-induced extinction such as non-density-dependent transmission (Rachowicz and Briggs 2007, Orlofske et al. 2018), reservoir hosts (McMahon et al. 2013), and small equilibrium densities (De Castro and Bolker 2005).

Although between-population differences in Bd load provide a straightforward explanation for the lower survival of infected adults at Subalpine compared to Alpine (Briggs et al. 2010), it is less obvious why uninfected adults also had lower survival at Subalpine. Low uninfected survival may result from differences in habitat characteristics and/or the abundance of terrestrial or aquatic predators that prey on adult frogs. For example, in 2013 ten translocated frogs at each site were tracked for several weeks using radiotelemetry. At Subalpine, two of these frogs were preyed on by garter snakes (*Thamnophis elegans* (Jennings et al. 1992)), and no evidence of predation was observed at Alpine.

We found that infected adults were easier to detect than uninfected adults, and at Alpine, infection load increased detection probability among infected individuals. This could relate to infection-related behavior that makes frogs easier to find and/or capture (Johnson 2002). For example, some amphibians increase feeding activity when infected with Bd (Hess et al. 2015). If this is the case for *R. sierrae*, we might expect frogs to spend more time around the lake edge, where they would be more conspicuous to observers. Some previous studies have assumed equal detectability among infected and uninfected frogs (Briggs et al. 2010, Stegen et al. 2017), while others have not (Retallick et al. 2004, Murray et al. 2009, Phillott et al. 2013). Our results indicate that even accounting for unequal detectability between uninfected and infected animals may not be sufficient, because Bd load may further affect detectability among infected individuals. Future studies should evaluate conditions under which disease impacts on detectability could bias estimates of demographic rates in wild populations.

The recruitment model developed here may be somewhat simplistic in its focus on adults. In reality, recruitment into the adult population is a function of dynamics in the subadult and larval populations. In particular, in mountain yellow-legged frogs and many other frog species Bd infection imposes heavy mortality during metamorphosis (Rachowicz and Vredenburg 2004, Rachowicz et al. 2006). Therefore, to fully understand how climate and disease influence population dynamics by way of affecting larvae, subadults, and adults, future efforts might focus on incorporating elements of integral projection models (Wilber et al. 2016) and integrated population models (Schaub and Abadi 2011) with hidden Markov models similar to those we developed in this study. A joint model for larval, subadult, and adult population dynamics would be better able to account for time lags resulting from the 1- to 4-yr larval development period of this species (Vredenburg et al. 2005). For example, one severe winter could have long-lasting effects if it slows the development of larvae so that they develop in three rather than two years, but this effect might not be detectable as a signal for adult recruitment until four years after the severe winter, depending on the growth rate of subadult frogs.

Our results provide important insights into causes of population establishment or likely failure for the endangered *R. sierrae*. The two study populations showed very different patterns of adult survival and recruitment, and in particular,

within a population the estimated survival of introduced cohorts was remarkably consistent across all introductions. Although the generality of results obtained from these two populations needs to be assessed using data from mark–recapture efforts at other reintroduced populations, the results suggest that the estimated survival of reintroduced frogs could provide an early indication of the site-specific probability of introduction success. Such indications could inform efficient allocation of limited conservation resources toward efforts that are likely to lead to persistent populations. In the future, when survival estimates of reintroduced frogs are available from a larger number of populations, these estimates could eventually allow the identification of site characteristics associated with likely introduction success or failure. This predictive ability would greatly increase the effectiveness of mountain yellow-legged frog recovery efforts.

More broadly, this work points to introduction of amphibian populations decimated by Bd as a potentially viable conservation action. Some introductions in other systems have failed due to chytridiomycosis (Stockwell et al. 2008, Soorae 2010), but the successful introduction of *R. sierrae* in Yosemite provides evidence that introductions can succeed even when Bd persists. Given the ongoing efforts to captively breed and then reintroduce threatened amphibians (Brannelly et al. 2016, Klop-Toker et al. 2016, Murphy and Gratwicke 2017), it is imperative to quantify the effects of Bd on host populations using imperfect observational data. It is our hope that the framework developed here can be leveraged to better understand factors determining introduction success, and to develop more effective conservation interventions.

Acknowledgments

We thank the following people and institutions for important contributions to this study: numerous people who assisted with the fieldwork (especially N. Kauffman, A. Killion, A. Lindauer, J. Maurer, and S. Ostoja); R. Chen, K. Rose, and M. Toothman for qPCR assistance; M. Wilber for reviewing an earlier draft of the manuscript; and Yosemite National Park (R. Grasso, H. McKenny, and S. Thompson), U.S. Geological Survey - Western Ecological Research Center (M. Brooks and S. Ostoja), and the University of California Natural Reserve System - Sierra Nevada Aquatic Research Laboratory (https://doi.org/10.21973/n3966f) for logistical support and valuable discussions. Research permits were provided by Yosemite National Park, U.S. Fish and Wildlife Service, and the Institutional Animal Care and Use Committee at the University of California, Santa Barbara. This project was funded by grants from the National Park Service (to R.A.K), Yosemite Conservancy (to Yosemite National Park and R.A.K.), U.S. Geological Survey (Ecosystems Mission Area - Natural Resource Preservation Program, to M. Brooks and R. Knapp for the project titled "Factors influencing reintroduction success of the endangered mountain yellow-legged frog"), and National Science Foundation (DEB-1557190, to C. Briggs and R. Knapp). We also thank H. Ito for translating mark–recapture model specifications from JAGS to Stan, as this greatly simplified our implementation. R.A.K. designed and performed the research and assembled and maintained the study data set; M.B.J. and R.A.K. developed the models and wrote the manuscript; and M.B.J. analyzed the data. The authors contributed equally to this work.

Literature Cited

Allaire, J., Y. Xie, J. McPherson, J. Luraschi, K. Ushey, A. Atkins, H. Wickham, J. Cheng and W. Chang. 2018. rmarkdown: dynamic documents for R. https://CRAN.R-project.org/package=rmarkdown

Armstrong, D. P., and P. J. Seddon. 2008. Directions in reintroduction biology. Trends in Ecology and Evolution 23:20–25.

Arnold, J. B. 2018. ggthemes: extra themes, scales and geoms for 'ggplot2'. https://CRAN.R-project.org/package=ggthemes

Boettiger, C. 2015. An introduction to Docker for reproducible research. ACM SIGOPS Operating Systems Review 49:71–79.

Boyle, D., D. Boyle, V. Olsen, J. Morgan, and A. Hyatt. 2004. Rapid quantitative detection of chytridiomycosis (*Batrachochytrium dendrobatidis*) in amphibian samples using real-time Taqman PCR assay. Diseases of Aquatic Organisms 60:141–148.

Brannelly, L. A., D. Hunter, L. F. Skerratt, B. Scheele, D. Lenger, M. S. McFadden, P. S. Harlow, and L. Berger. 2016. Chytrid infection and post-release fitness in the reintroduction of an endangered alpine tree frog. Animal Conservation 19:153–162.

Briggs, C. J., R. A. Knapp, and V. T. Vredenburg. 2010. Enzootic and epizootic dynamics of the chytrid fungal pathogen of amphibians. Proceedings of the National Academy of Sciences USA 107:9695–9700.

Carpenter, B., A. Gelman, M. Hoffman, D. Lee, B. Goodrich, M. Betancourt, M. A. Brubaker, J. Guo,

P. Li, and A. Riddell. 2016. Stan: a probabilistic programming language. Journal of Statistical Software 20:1–37.

Cohen, J. M., M. D. Venesky, E. L. Sauer, D. J. Civitello, T. A. McMahon, E. A. Roznik, and J. R. Rohr. 2017. The thermal mismatch hypothesis explains host susceptibility to an emerging infectious disease. Ecology Letters 20:184–193.

Conn, P. B., and E. G. Cooch. 2009. Multistate capture–recapture analysis under imperfect state observation: an application to disease models. Journal of Applied Ecology 46:486–492.

De Castro, F., and B. Bolker. 2005. Mechanisms of disease-induced extinction. Ecology Letters 8:117–126.

Dennis, E. B., B. J. Morgan, and M. S. Ridout. 2015. Computational aspects of N-mixture models. Biometrics 71:237–246.

Drost, C. A., and G. M. Fellers. 1996. Collapse of a regional frog fauna in the Yosemite area of the California Sierra Nevada, USA. Conservation Biology 10:414–425.

Fellers, G. M., D. E. Green, and J. E. Longcore. 2001. Oral chytridiomycosis in the mountain yellow-legged frog (*Rana muscosa*). Copeia 2001:945–953.

Fisher, M. C., T. W. Garner, and S. F. Walker. 2009. Global emergence of *Batrachochytrium dendrobatidis* and amphibian chytridiomycosis in space, time, and host. Annual Review of Microbiology 63:291–310.

Ford, J. H., M. V. Bravington, and J. Robbins. 2012. Incorporating individual variability into mark–recapture models. Methods in Ecology and Evolution 3:1047–1054.

Gimenez, O., and R. Choquet. 2010. Individual heterogeneity in studies on marked animals using numerical integration: capture–recapture mixed models. Ecology 91:951–957.

Grant, E. H. C., et al. 2016. Quantitative evidence for the effects of multiple drivers on continental-scale amphibian declines. Scientific Reports 6:25625.

Grolemund, G., and H. Wickham. 2011. Dates and times made easy with lubridate. Journal of Statistical Software 40:1–25.

Hess, A., C. McAllister, J. DeMarchi, M. Zidek, J. Murone, and M. D. Venesky. 2015. Salamanders increase their feeding activity when infected with the pathogenic chytrid fungus *Batrachochytrium dendrobatidis*. Diseases of Aquatic Organisms 116:205–212.

Hudson, M. A., et al. 2016. In-situ itraconazole treatment improves survival rate during an amphibian chytridiomycosis epidemic. Biological Conservation 195:37–45.

Hyatt, A. D., et al. 2007. Diagnostic assays and sampling protocols for the detection of *Batrachochytrium dendrobatidis*. Diseases of Aquatic Organisms 73:175–192.

IUCN. 2017. The IUCN red list of threatened species. version 2017-3. http://www.iucnredlist.org

Jennings, W. B., D. F. Bradford, and D. F. Johnson. 1992. Dependence of the garter snake *Thamnophis elegans* on amphibians in the Sierra Nevada of California. Journal of Herpetology 26:503–505.

Johnson, R. 2002. The concept of sickness behavior: a brief chronological account of four key discoveries. Veterinary Immunology and Immunopathology 87:443–450.

Jolly, G. M. 1965. Explicit estimates from capture-recapture data with both death and immigration-stochastic model. Biometrika 52:225–247.

Joseph, M. B. and R. A. Knapp. 2018. SNARL1/sierra-reintroduction-cmr: initial release. https://doi.org/10.5281/zenodo.1253754

Klop-Toker, K., J. Valdez, M. Stockwell, L. Fardell, S. Clulow, J. Clulow, and M. Mahony. 2016. We made your bed, why won't you lie in it? Food availability and disease may affect reproductive output of reintroduced frogs. PLoS ONE 11:e0159143.

Knapp, R. A. 2005. Effects of nonnative fish and habitat characteristics on lentic herpetofauna in Yosemite National Park, USA. Biological Conservation 121:265–279.

Knapp, R. A., C. J. Briggs, T. C. Smith, and J. R. Maurer. 2011. Nowhere to hide: impact of a temperature-sensitive amphibian pathogen along an elevation gradient in the temperate zone. Ecosphere 2:1–26.

Knapp, R. A., G. M. Fellers, P. M. Kleeman, D. A. Miller, V. T. Vredenburg, E. B. Rosenblum, and C. J. Briggs. 2016. Large-scale recovery of an endangered amphibian despite ongoing exposure to multiple stressors. Proceedings of the National Academy of Sciences USA 113:11889–11894.

Knapp, R. A., and K. R. Matthews. 2000. Non-native fish introductions and the decline of the mountain yellow-legged frog from within protected areas. Conservation Biology 14:428–438.

Kriger, K. M., J.-M. Hero, and K. J. Ashton. 2006. Cost efficiency in the detection of chytridiomycosis using PCR assay. Diseases of Aquatic Organisms 71:149–154.

Kucukelbir, A., R. Ranganath, A. Gelman, and D. Blei. 2015. Automatic variational inference in Stan. Pages 568–576 *in* C. Cortes, N. D. Lawrence, D. D. Lee, M. Sugiyama, and R. Garnett, editors. Advances in neural information processing systems. Curran Associates, Red Hook, New York, USA.

Lebreton, J., and R. P. Cefe. 2002. Multistate recapture models: modelling incomplete individual histories. Journal of Applied Statistics 29:353–369.

Lindenmayer, D., and B. Scheele. 2017. Do not publish. Science 356:800–801.

Longo, A. V., D. Rodriguez, D. da Silva Leite, L. F. Toledo, C. M. Almeralla, P. A. Burrowes, and K. R. Zamudio. 2013. ITS1 copy number varies among *Batrachochytrium dendrobatidis* strains: implications for qPCR estimates of infection intensity from field-collected amphibian skin swabs. PLoS ONE 8:e59499.

McCallum, H., and A. Dobson. 1995. Detecting disease and parasite threats to endangered species and ecosystems. Trends in Ecology and Evolution 10:190–194.

McMahon, T. A., L. A. Brannelly, M. W. Chatfield, P. T. Johnson, M. B. Joseph, V. J. McKenzie, C. L. Richards-Zawacki, M. D. Venesky, and J. R. Rohr. 2013. Chytrid fungus *Batrachochytrium dendrobatidis* has nonamphibian hosts and releases chemicals that cause pathology in the absence of infection. Proceedings of the National Academy of Sciences USA 110:210–215.

Miller, D. A., B. L. Talley, K. R. Lips, and E. H. Campbell Grant. 2012. Estimating patterns and drivers of infection prevalence and intensity when detection is imperfect and sampling error occurs. Methods in Ecology and Evolution 3:850–859.

Murphy, J. B., and B. Gratwicke. 2017. History of captive management and conservation amphibian programs mostly in zoos and aquariums. Part I-Anurans. Herpetological Review 48:241–260.

Murray, K. A., L. F. Skerratt, R. Speare, and H. McCallum. 2009. Impact and dynamics of disease in species threatened by the amphibian chytrid fungus, *Batrachochytrium dendrobatidis*. Conservation Biology 23:1242–1252.

Orlofske, S. A., S. M. Flaxman, M. B. Joseph, A. Fenton, B. A. Melbourne, and P. T. Johnson. 2018. Experimental investigation of alternative transmission functions: quantitative evidence for the importance of nonlinear transmission dynamics in host–parasite systems. Journal of Animal Ecology 87:703–715.

Pedersen, T. L. 2017. patchwork: the composer of ggplots. https://github.com/thomasp85/patchwork

Phillips, K. 1990. Where have all the frogs and toads gone? BioScience 40:422–425.

Phillott, A. D., L. F. Grogan, S. D. Cashins, K. R. McDonald, L. Berger, and L. F. Skerratt. 2013. Chytridiomycosis and seasonal mortality of tropical stream-associated frogs 15 years after introduction of *Batrachochytrium dendrobatidis*. Conservation Biology 27:1058–1068.

Pilliod, D. S., E. Muths, R. D. Scherer, P. E. Bartelt, P. S. Corn, B. R. Hossack, B. A. Lambert, R. McCaffery, and C. Gaughan. 2010. Effects of amphibian chytrid fungus on individual survival probability in wild boreal toads. Conservation Biology 24:1259–1267.

Pledger, S., K. H. Pollock, and J. L. Norris. 2003. Open capture-recapture models with heterogeneity: I. Cormack-Jolly-Seber model. Biometrics 59:786–794.

Pradel, R. 1996. Utilization of capture-mark-recapture for the study of recruitment and population growth rate. Biometrics 52:703–709.

R Core Team. 2017. R: a language and environment for statistical computing. R Foundation for Statistical Computing, Vienna, Austria.

Råberg, L., A. L. Graham, and A. F. Read. 2009. Decomposing health: tolerance and resistance to parasites in animals. Philosophical Transactions of the Royal Society B: Biological Sciences 364:37–49.

Rachowicz, L. J., and C. J. Briggs. 2007. Quantifying the disease transmission function: effects of density on *Batrachochytrium dendrobatidis* transmission in the mountain yellow-legged frog *Rana muscosa*. Journal of Animal Ecology 76:711–721.

Rachowicz, L. J., R. A. Knapp, J. A. Morgan, M. J. Stice, V. T. Vredenburg, J. M. Parker, and C. J. Briggs. 2006. Emerging infectious disease as a proximate cause of amphibian mass mortality. Ecology 87:1671–1683.

Rachowicz, L. J., and V. T. Vredenburg. 2004. Transmission of *Batrachochytrium dendrobatidis* within and between amphibian life stages. Diseases of Aquatic Organisms 61:75–83.

Retallick, R. W., H. McCallum, and R. Speare. 2004. Endemic infection of the amphibian chytrid fungus in a frog community post-decline. PLoS Biology 2:e351.

Royle, J. A. 2008. Modeling individual effects in the Cormack–Jolly–Seber model: a state–space formulation. Biometrics 64:364–370.

Royle, J. A. 2009. Analysis of capture–recapture models with individual covariates using data augmentation. Biometrics 65:267–274.

Royle, J. A., and R. M. Dorazio. 2012. Parameter-expanded data augmentation for Bayesian analysis of capture–recapture models. Journal of Ornithology 152:521–537.

Sapsford, S. J., M. J. Voordouw, R. A. Alford, and L. Schwarzkopf. 2015. Infection dynamics in frog populations with different histories of decline caused by a deadly disease. Oecologia 179:1099–1110.

Schaub, M., and F. Abadi. 2011. Integrated population models: a novel analysis framework for deeper insights into population dynamics. Journal of Ornithology 152:227–237.

Sherman, C. K., and M. L. Morton. 1993. Population declines of Yosemite toads in the eastern Sierra Nevada of California. Journal of Herpetology 27:186–198.

Sinsch, U. 1984. Thermal influences on the habitat preference and the diurnal activity in three European *Rana* species. Oecologia 64:125–131.

Skerratt, L. F., L. Berger, R. Speare, S. Cashins, K. R. McDonald, A. D. Phillott, H. B. Hines, and N. Kenyon. 2007. Spread of chytridiomycosis has caused

the rapid global decline and extinction of frogs. EcoHealth 4:125–134.

Slowikowski, K. 2017. ggrepel: repulsive text and label geoms for 'ggplot2'. https://CRAN.R-project.org/package=ggrepel

Soorae, P. S. 2010. Global re-introduction perspectives: additional case studies from around the globe. IUCN/SSC Re-introduction Specialist Group & Environment Agency-Abu Dhabi, United Arab Emirates.

Spitzen-van der Sluijs, A., S. Canessa, A. Martel, and F. Pasmans. 2017. Fragile coexistence of a global chytrid pathogen with amphibian populations is mediated by environment and demography. Proceedings of the Royal Society of London B: Biological Sciences 284:20171444.

Stallman, R. M., R. McGrath, and P. D. Smith. 2004. GNU Make: a program for directing recompilation, for version 3.81. Free Software Foundation, Boston, Massachusetts, USA.

Stan Development Team. 2016. RStan: the R interface to Stan. https://cran.r-project.org/package=rstan

Stegen, G., et al. 2017. Drivers of salamander extirpation mediated by *Batrachochytrium salamandrivorans*. Nature 544:353.

Stockwell, M., S. Clulow, J. Clulow, and M. Mahony. 2008. The impact of the amphibian chytrid fungus *Batrachochytrium dendrobatidis* on a green and golden bell frog *Litoria aurea* reintroduction program at the Hunter Wetlands Centre Australia in the Hunter Region of NSW. Australian Zoologist 34:379–386.

Vredenburg, V. T., R. Bingham, R. Knapp, J. A. Morgan, C. Moritz, and D. Wake. 2007. Concordant molecular and phenotypic data delineate new taxonomy and conservation priorities for the endangered mountain yellow-legged frog. Journal of Zoology 271:361–374.

Vredenburg, V. T., G. M. Fellers, and C. Davidson. 2005. The mountain yellow-legged frog (*Rana muscosa*). Pages 563–566 *in* M. J. Lannoo, editor. Amphibian declines: the conservation status of United States species. University of California Press, Berkeley, California, USA.

Vredenburg, V. T., R. A. Knapp, T. S. Tunstall, and C. J. Briggs. 2010. Dynamics of an emerging disease drive large-scale amphibian population extinctions. Proceedings of the National Academy of Sciences USA 107:9689–9694.

Wake, D. B., and V. T. Vredenburg. 2008. Are we in the midst of the sixth mass extinction? A view from the world of amphibians. Proceedings of the National Academy of Sciences USA 105:11466–11473.

Wickham, H. 2007. Reshaping data with the reshape package. Journal of Statistical Software 21:1–20.

Wickham, H. 2017*a*. assertthat: easy pre and post assertions. https://CRAN.R-project.org/package=assertthat

Wickham, H. 2017*b*. tidyverse: Easily install and load the 'tidyverse'. https://CRAN.R-project.org/package=tidyverse

Wilber, M. Q., R. A. Knapp, M. Toothman, and C. J. Briggs. 2017. Resistance, tolerance and environmental transmission dynamics determine host extinction risk in a load-dependent amphibian disease. Ecology Letters 20:1169–1181.

Wilber, M. Q., K. E. Langwig, A. M. Kilpatrick, H. I. McCallum, and C. J. Briggs. 2016. Integral projection models for host–parasite systems with an application to amphibian chytrid fungus. Methods in Ecology and Evolution 7:1182–1194.

Wilke, C. O. 2018. ggridges: ridgeline plots in 'ggplot2'. https://CRAN.R-project.org/package=ggridges

Wood, S. N. 2004. Stable and efficient multiple smoothing parameter estimation for generalized additive models. Journal of the American Statistical Association 99:673–686.

Wood, S. N. 2017. Generalized additive models: an introduction with R. Chapman & Hall/CRC, Boca Raton, Florida, USA.

Zucchini, W., I. L. MacDonald, and R. Langrock. 2016. Hidden Markov models for time series: an introduction using R. Chapman & Hall/CRC, Boca Raton, Florida, USA.

Supporting Information

Additional Supporting Information may be found online at: http://onlinelibrary.wiley.com/doi/10.1002/ecs2.2499/full